Top Catal (2015) 58:258–270
DOI 10.1007/s11244-015-0367-z

ORIGINAL PAPER

# Use of Solvatochromism to Assay Preferential Solvation of a Prototypic Catalytic Site

**Birgit Schwenzer · Lelia Cosimbescu · Vassiliki-Alexandra Glezakou · Abhijeet J. Karkamkar · Zheming Wang · Robert S. Weber**

Published online: 6 March 2015


**Abstract** The composition of the reaction medium near photoactive catalytic sites can be inferred from the solvatochromism of the absorption and emission spectra of the wetted sites, which depend on the polarizability of the fluid. In brief, solvatochromism measures the interaction of the dipole moments of the ground and excited states with the electric field imposed by the solvent shell: a field, which does not relax on the time scale of the absorption or emission events. To establish the utility of the technique for inorganic catalysts that operate in complex reaction media, such as encountered in the upgrading of biogenic fuels, we have measured the solvatochromism of a common, structural feature of metal oxide catalysts, monooxide or dioxide of a transition metal prepared by incorporating the OM or $O_2M$ moiety into the framework of a polyhedral oligomeric silsesquioxane (POSS). In toluene, cyclohexene, chloroform and tetrahydrofuran, POSS-ligated oxometalates exhibit strong ligand-to-metal charge-transfer bands in their UV–visible absorption and emission spectra. From the solvatochromism of the chromophores dissolved in toluene-chloroform mixtures we inferred an unexpectedly strong, preferential solvation of the chromophore even when all three components (oxometalate and the two solvents) were highly miscible.

B. Schwenzer · Z. Wang
Physical Sciences Division, Pacific Northwest National Laboratory, P.O. Box 999, Richland, WA 99352, USA

L. Cosimbescu · V.-A. Glezakou · A. J. Karkamkar · R. S. Weber (✉)
Institute for Integrated Catalysis, Pacific Northwest National Laboratory, P.O. Box 999 MS-IN K2-12, Richland, WA 99352, USA
e-mail: robert.weber@pnnl.gov

*Graphical Abstract*

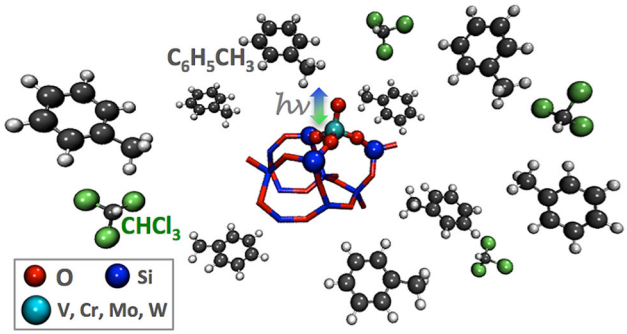


**Keywords** Luminescence spectroscopy vanadium · Chromium · Molybdenum · Tungsten oxides · TD-DFT · Ligand-to-metal charge transfer spectroscopy · Mesoscale measurements

## 1 Introduction

Solvent effects on reaction rates have a long history in catalysis [1–7]. The conventional rationalizations of solvent effects in catalysis include the modification of the solubility of reactants and products [5, 8], the modification of transport rates [8] and the effects of solvent on the adsorption of reactants [2], products [9] and the solvent itself [1]. Interest in solvent effects has increased recently [8, 10, 11] to contend with the complexity of the reaction media that arise in the catalytic processing into fuels of biogenic feedstocks, particularly those prepared from thermochemically produced biogenic feedstocks (pyrolysis oil). Pyrolysis oil usually presents initially as a blend of both polar and nonpolar compounds that transforms with

increasing hydroprocessing into segregated layers of oil and water.

When a reaction medium contains components of widely differing polarizability, the composition and dynamics of a catalyst's cybotactic region (solvent immediately adjacent to the active sites) may differ from the average composition of the bulk fluid. In the hydroprocessing of biogenic fuels, it would be useful to understand the nature of the reaction medium adjacent to the catalyst. Similarly in Fischer–Tropsch synthesis the reaction mixture may wet the catalyst differently as a function of conversion because the hydrocarbon molecules comprising the target fuel are nonpolar (relative permittivity, $\varepsilon \lesssim 2$) while water and intermediate oxygenates water are strong to moderate dielectrics ($10 \leq \varepsilon \leq 80$). Very localized solvent gradients could also be present in reactions occurring in more conventional solvent mixtures [12–14] or ionic liquids [15] even in the absence of transport limitations that can create concentration gradients, and possibly well before the separation of immiscible reactant and product phases that occurs at high conversion. Such a thermodynamically driven segregation could arise either from preferential solvation of the sites themselves or from solvent structuring that propagates from the surface of the catalyst support. The local structuring of the solvent could affect reaction selectivities and rates by altering the energies of reaction intermediates and transition states, and would depend on interactions whose characteristic energies and dynamics lie between those of strong ligation and the solvent–solvent interactions of the bulk fluid.

Solvatochromism [16] or, more generally, perichromism [17] (effect of the surrounding medium on the Stokes shifts between absorption and emission maxima) has proved useful in biology [16] and in rheology [18] for probing compositional variations and fluid mobility at length scales of around 1 nm [19], comparable to what we envisage for stratification of multiphasic reaction media in the pores of heterogeneous catalysts [20]. UV–visible spectroscopy of surface species is well established for studying catalysts [15, 21–27] and perichromism of indicator dyes has also been used to characterize solid surfaces and catalysts [17, 19, 28–34]. However, we could find no report of the use of solvatochromism of surface-supported chromophores, or their analogs, to directly characterize the composition of the reaction medium adjacent to the sites of heterogeneous catalysts, such as might eventually be deployed *in operando*.

In brief, solvatochromism arises when the dipole moments of the ground state ($\mu_G$) and excited state ($\mu_E$) of a chromophore differ in magnitude and orientation such that the energies of absorption ($h\nu_A$) and fluorescence ($h\nu_F$) are differentially stabilized by the polarizability of the surrounding molecules, whose relaxations are slow on the time scale of the (vertical) absorption and emission events (Fig. 1). Although there are many refinements [16, 35–38], the effect of the solvent on the difference in energy between absorption and emission can often be correlated, through Lippert's Relation [39], with the properties of the chromophore (changes in its dipole moment upon excitation ($\mu_G - \mu_E$), radius of the cavity ($a$) it makes in the solvent), and the properties of the solvent (orientation polarizability, $\Delta f$):

$$h\nu_A - h\nu_F = \frac{2}{c}\Delta f \frac{(\mu_E - \mu_G)^2}{a^3}, \quad (1)$$

where the orientation polarizability of the environment depends on the relative permittivity of the medium, $\varepsilon$, and its index of refraction, $n$:

$$\Delta f = \frac{\varepsilon - 1}{2\varepsilon + 1} - \frac{n^2 - 1}{2n^2 + 1}. \quad (2)$$

As a first step towards determining the effects of the solid surface of a heterogeneous catalyst and its porosity on the structure and composition on the liquid phase adjacent to the catalyst sites, we measured the solvatochromism of a series of homogeneous *model* compounds (Fig. 2). The model complexes were charge-transfer chromophores prepared using established or analogous literature recipes to ligate oxometalates of V, Cr, Mo and W, with lacunary, polyhedral oligomeric silsesquioxane (POSS). These POSS-ligated oxometalates exhibit UV–Visible absorption spectra similar to those of the surface-supported moieties but the complexes dissolve in common solvents to form readily analyzable solutions. POSS-ligated oxometalates have proven to be close mimics of the spectroscopic and catalytic behaviors of their silica-supported analogs [40]

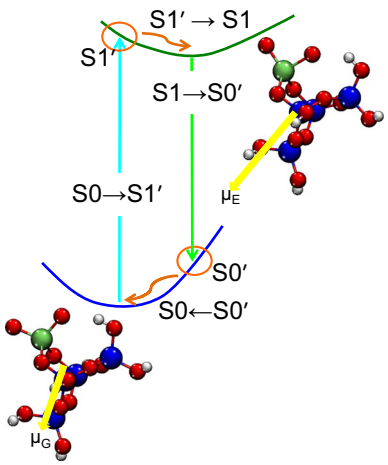


**Fig. 1** Schematic of vertical absorption and emission processes among the ground state, $S_0$, the unrelaxed excited state $S_1'$, the relaxed excited state $S_1$ and the unrelaxed ground state $S_0'$. The *block arrows* represent the dipole vectors of the molecules in the ground and excited states

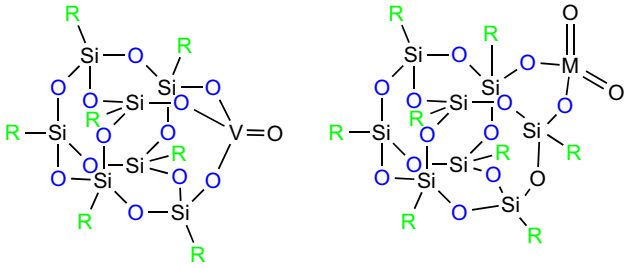

**Fig. 2** Schematics of the mono-oxo (*left* R = phenyl) and dio-oxo POSS-ligated complexes (*right* R = isobutyl); M = Cr, Mo, or W

and they are seeing increased use as model catalysts [41, 42] and as precursors to catalysts [43, 44].

We report here the construction and interpretation of prototypic calibration curves that assay the composition of a liquid medium near a moiety that resembles the presumed active site in silica-supported oxide catalysts, which are well known as catalysts for polymerization [45], selective oxidation [46], metathesis [47], and photolysis [48].

## 2 Materials and Methods

### 2.1 Materials

Oxo anions of vanadium, molybdenum and tungsten were prepared by the reaction of equimolar oxychlorides with trihydroxyphenyl $T_7$ polysilsesquioxane (V) or dihydroxyisobutyl $T_7$ silsesquioxane (Mo, W) complexes [49–51]. A chromium analog was prepared starting with chromium trioxide (see "Appendix" section for details). The reactions were carried out under inert atmosphere in dry toluene. Triethylamine was added to the reaction mixture to precipitate HCl produced during the reaction, as $Et_3NHCl$. The vanadyl species was obtained as a monoxovanadate in the +5 oxidation state; the Cr, Mo and W species were prepared as dioxometalate species with the metal in the +6 oxidation state. The resulting materials were characterized by solution $^{29}Si$, $^{1}H$ and $^{13}C$ NMR, and mass spectroscopy. The OVPOSS species was also characterized by $^{51}V$ NMR. The vanadium analog was also prepared via an additional method with equimolar vanadium oxytripropoxide in benzene, without the addition of triethylamine, in an effort to improve the purity and isolation of the product (see "Appendix" section for details). The results of the analyses were consistent with the expected geometries of the POSS-ligated complexes, monometallic complexes in all cases except for the vanadyl complex, which was obtained as a mixture of the mono vanadium complex and its corresponding dimer (see "Appendix" section for details).

#### *2.1.1 Solvents*

The solvents (toluene, cyclohexene, chloroform and tetrahydrofuran) were spectroscopy grade used either as received or, if necessary, after drying by passage through columns of activated alumina. We estimated the orientation polarizablities of the solvents and solvent mixtures from measurements of their indices of refraction and values for their dielectric constants calculated according to the algorithm described by Wang and Anderko [52] (see Table 3).

### 2.2 Spectroscopy

#### *2.2.1 In Neat Solvents*

Stock solutions of the complexes (OVPOSS, $O_2$CrPOSS, $O_2$MoPOSS and $O_2$WPOSS) were prepared by dissolution of calculated weights of the complexes in the chosen solvents and dilution to yield ~8–10 μM solutions. The concentrations of the individual solutes were adjusted to an absorbance of approximately 0.5, therefore the actual concentration of the individual samples depended on the absorption coefficient of the parent POSS-ligated complex in the specific solvent. UV/Vis absorption spectra of the solutions contained in screw-capped quartz cuvettes were recorded at room temperature (23 °C) using a Shimadzu UV 3600 UV–Vis-near infrared (NIR) Spectrometer. All spectra were baseline corrected against the pure solvents and acquired with a resolution of 0.5 nm over the range 200–800 nm. Emission spectra were measured using a Horiba FluoroMax-4 Spectrofluorometer in combination with the manufacturer supplied FluorEssence software (version 3.5). The measurements were recorded with a resolution of 1 nm and averaged over five acquisitions (5 nm bandpass on both the front entrance slit and the front exit slit). The previously determined absorption maximum for each respective complex was used as the excitation wavelength; dark offset and blank subtraction corrections were applied to each spectrum. The recorded wavelength range for the spectra depended on the excitation wavelength that was used.

#### *2.2.2 Toluene–Chloroform Solutions*

The complexes were dissolved in solvent mixtures consisting of different ratios of toluene and chloroform, spanning a range from 0 to 100 vol% chloroform. Absorption and emission spectra were recorded as described above, except that the energy of the absorption maximum of each complex in toluene was used as the excitation energy for all samples of the same complex. For example, each spectrum in the series of emission spectra for OVPOSS was recorded using the excitation energy of

4.428 eV (280 nm) (see Fig. 10). As a control, we also used the energy of the absorption maxima of the chromophores dissolved in pure chloroform as the excitation energy for the emission spectra. However, we did not observe any evidence that the emission spectral profiles were influenced by the change in the excitation energy.

#### 2.2.3 *Measurements at 50 °C*

$O_2$WPOSS was dissolved in solution mixtures consisting of different volumetric ratios of toluene to chloroform as described above. The Horiba FluoroMax-4 Spectrofluorometer was equipped with a water-heated cuvette holder that permitted recording emission spectra of these samples at elevated temperature. The cuvette holder was maintained at a temperature between 48.5 and 49.8 °C during the measurements, with the aid of a programmable circulating bath, set to 50 °C. Prior to the measurement, the quartz cuvettes containing $O_2$WPOSS dissolved in toluene–chloroform solution mixtures were preconditioned in a convection oven at ~45 °C to ensure that the actual sample would reach the desired temperature for the measurement (~50 °C) within a reasonable time frame, and to keep temperature variations between the samples at a minimum. The actual emission measurements were carried out as described above.

### 2.3 Modeling

In this study, the full geometry of the POSS-ligated complexes was approximated with smaller silica fragments terminated with hydrogen atoms (Fig. 3). Full geometry optimizations of the lowest singlet spin states for all systems were carried out with density functional theory (DFT) using the 1998 revised Perdue-Burke-Ernzerhof hybrid functional (PBE0) [53]. This functional, in combination with time dependent-DFT (TD-DFT), has been shown to produce fairly accurate and inexpensive predictions of optical excitations for transition metal systems [54]. A double zeta quality basis set with polarization functions was used for the main group elements (H, C, O, and Si). The Stuttgart effective core potentials with the companion double-zeta quality basis sets were used for the transition metals V, Cr, Mo and W. All equilibrium geometries were verified by Hessian calculations. Tests with bigger silica clusters gave directionally similar results (within 0.5 eV) for the oxo-metalate moiety; so we used the smaller clusters to save the computational costs for the excited state calculations. Vertical excitations to the lowest singlet excited state and "diagonal" excitations were determined using time-dependent DFT (TD-DFT [55] ) as implemented in Gaussian 09 [56]. The "diagonal" excitations (ground state minima to excited state minima) were determined by full optimization of the lowest singlet excited states.

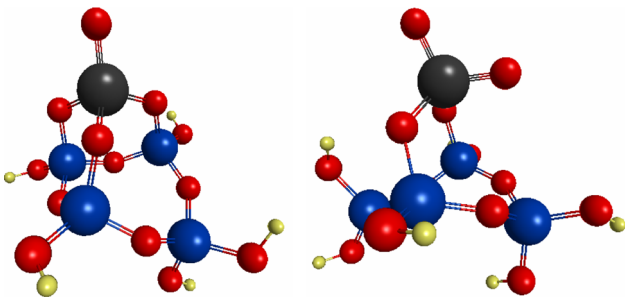

**Fig. 3** Clusters used in the quantum chemical modeling. *Left* silica-ligated unioxo vanadyl, *Right* silica-ligated dioxo complexes of Cr, Mo, W

We incorporated solvent effects by means of a polarizable continuum model (PCM) by placing the clusters in a cavity within the solvent reaction field [55, 57] determined by the dielectric of the solvent, i.e. chloroform ($\varepsilon = 4.7113$) and toluene ($\varepsilon = 2.3741$). Vertical and "diagonal" excitations were also obtained with the PCM approach for all systems.

## 3 Results and Discussion

The absorption of the POSS-ligated compounds dissolved in toluene, a nonpolar solvent with a small solvatochromic effect, exhibited absorption maxima at energies typical of those found for isolated, supported oxometalates (Table 1) [24]. Similarly, the calculated values were comparable to the experimentally measured energies, within the expected accuracy of the underlying theory and are expected to be of semi-quantitative value.

The spectra of the POSS complexes (see Appendix, Fig. 10) exhibited positive Stokes shifts (Fig. 4). We included in Fig. 4 a preliminary data point for the $O_2$-WPOSS complex impregnated into MCM-41 and then dried. The point lies along the extrapolation of the trend line towards an orientation polarizability of zero, just as would be expected for an environment with the low polarizability of air. Orientation polarizabilites were calculated using Eq. 2, using the procedure described in the "Appendix" section.

We used Lippert's Relation (Eq. 1) to calculate an apparent, relative change in the dipole moment between ground and excited states $\Delta\mu = (\mu_G - \mu_E)$ for the complexes dissolved in pure solvents. Comparison of our experimentally measured values for the Group VI chromophores with those that we calculated (Table 2) suggests that the photon absorption and emission we observed correspond, as might be expected, to the transfer of

**Table 1** Comparison of the measured and calculated energies for the absorption maxima of the POSS-ligated oxometalates with those of their silica-supported analogs

| Oxo species | Measured $E_{abs}$/eV for POSS-ligated oxo species in toluene | Calculated $E_{abs}$/eV for clusters in a polarizable continuum ($\varepsilon = 2.2$, viz. toluene) | Measured $E_{abs}$/eV of silica-supported oxo species [24], dried at 400 °C | Calculated $E_{abs}$/eV for clusters in vacuum |
|---|---|---|---|---|
| OV | 4.39 | 4.7 | 4.28 | 4.8 |
| $O_2Cr$ | 4.44 | 4.1 | 5.04 | 4.3 |
| $O_2Mo$ | 4.44 | 5.0 | 5.23 | 5.2 |
| $O_2W$ | 4.42 | 5.2 | 5.37 | 5.4 |

an electron from the ground-state singlet state to lowest excited singlet state and its reverse.

The calculated Stokes shifts (see Appendix, Table 4) trend oppositely to the experimental values, likely because they involve differences of differences and are therefore very sensitive to small errors. For transition metal complexes, we expected the calculated and experimental energies for the optical transitions to be within ~0.3 eV of their calculated values [54]. The discrepancy in the absorption energy is most pronounced for W, as might be expected for a late transition metals and our use of a moderately sized basis set [54, 58]. Better agreement would require the application of more refined, and much more expensive methods that take into account electron–electron correlations.

To investigate the possibility of preferential solvation that bears on nanoscopic phase separation outlined in the introduction, we measured the solvatochromism of the POSS complexes in solvent mixtures. In this initial study, we chose to use mixtures of toluene and chloroform as the binary solvents. In each case the spectra showed shifts consistent with a toluene-rich surrounding, even at concentrations of chloroform as high as 96 mol% (Fig. 5). The data were fit well by Langmuir-like isotherms that contained one fitting parameter, an apparent equilibrium constant, $K(T)$, to interpolate (partition) the composition (mol fraction), $X$, of the near-chromophore environment

**Table 2** Measured and calculated differences in the dipole moments for the ground and Franck–Condon excited state complexes (corresponding to the right term in Lippert's Relation), normalized, arbitrarily, to that of the $O_2$CrPOSS complex

| Sample | Measured relative Δμ | Calculated relative Δμ |
|---|---|---|
| OVPOSS | 0.4 | 0.8 |
| $O_2$CrPOSS | ≡1.0 | ≡1.0 |
| $O_2$MoPOSS | 0.9 | 1.2 |
| $O_2$WPOSS | 0.9 | 1.0 |

The measured dipole moments were calculated from the slope of the lines in Fig. 4. The calculated dipole moments were calculated as the vector difference between the dipole moments of the relaxed ground state and the unrelaxed (vertical) excited state for each complex

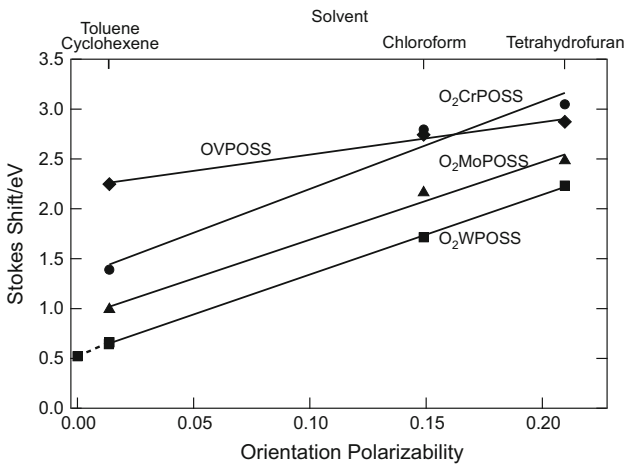


**Fig. 4** Solvatochromic stokes shifts of the POSS complexes dissolved in the neat solvents. The Stokes shifts were calculated as the difference in energy between the absorption peak and the emission peak for each solution. The emission spectra measured using the absorption maxima as the excitation energy

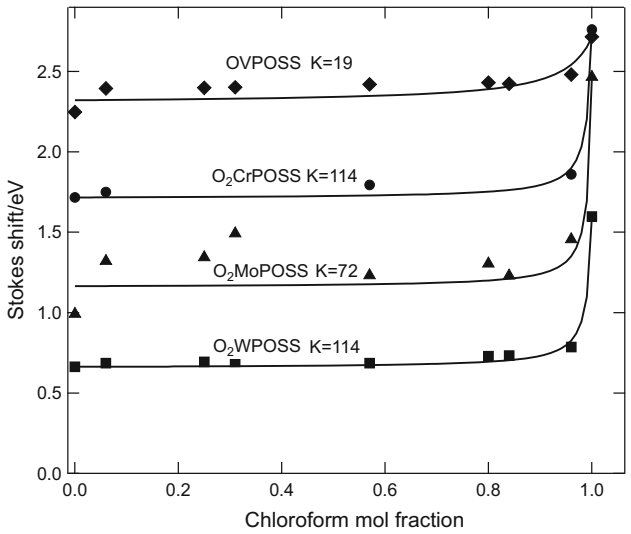


**Fig. 5** Stokes shifts for all the POSS complexes fitted with Langmuir-like isotherms corresponding to the indicated values for the partition constant, $K$

between toluene (Tol) and chloroform (Chl) as functions of the bulk composition of the solution (Eqs. 3–5):

$$X_{Tol} = \frac{K(T) \times X_{Tol\,bulk}}{X_{Chl\,bulk} + K(T) \times X_{Tol\,bulk}} \quad (3)$$

$$X_{Chl} = \frac{X_{Chl\,bulk}}{X_{Chl\,bulk} + K(T) \times X_{Tol\,bulk}} \quad (4)$$

$$Shift = X_{Tol} \times Shift_{Tol} \times X_{Chl} \times Shift_{Chl}. \quad (5)$$

This analysis is a 1-parameter simplification of that employed by Bosch, et al. [59]. We were surprised that the apparent equilibrium constants were large enough to yield such strong preferentiality given that the solvents are miscible [60] (toluene and chloroform have very similar enthalpies of vaporization, 33.2 and 29.2 kJ/mol, and very similar Hildebrand solubility parameters, 18.7 and 18.3 $MPa^{0.5}$). We did confirm that the solvent mixtures exhibited normal, concentration-dependent polarizabilities by demonstrating that the values of the Reichardt polarity indicator parameter [12], $E_T(30)$, for the solvatochromic benchmark, Reichardt's dye, were linearly dependent on the orientation polarizabilties of the mixtures (Fig. 6). Therefore, we are confident that the plateau region in the solvatochromism curves for the POSS complexes in mixtures of toluene and chloroform represent preferential solvation and not some instrumental or experimental artifact.

We recognize that much more complicated behavior of probe molecules in mixed solvents is possible because the interactions between probe and the solvent will depend on more than merely the bulk polarizability of the solvents [14, 16, 38, 39, 59, 61, 62]. We call attention to this simple analysis because, in our examination the literature on catalysis, we have found scant reference to the use of solvatochromism for characterizing the immediate environment of the catalyst, outside of enzyme catalysis.

For the preferential solvation to play a significant role in reactions, like the upgrading of biogenic fuels, it would need to persist to the temperatures where those reactions exhibit practicable rates, for example at temperatures greater than 250 °C. Therefore, we estimated the temperature dependence of preferential solvation depicted in Fig. 5 for the $O_2$WPOSS complex by also measuring and fitting its solvatochromism (Fig. 7) in the same solvent mixtures at 50 °C, which is about 10 °C below the boiling point of chloroform. A van't Hoff analysis of the apparent

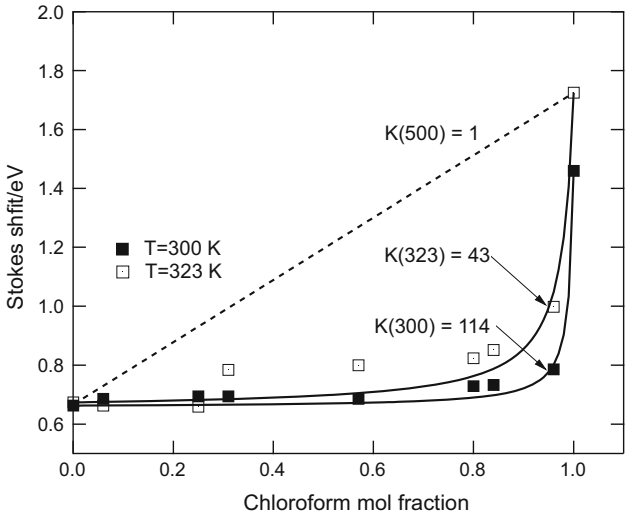


**Fig. 7** Solvatochromism of the $O_2$WPOSS complex measured at two temperatures. *Upper curve* shows the isotherm corresponding to a Langmuir equilibrium constant for partitioning of unity

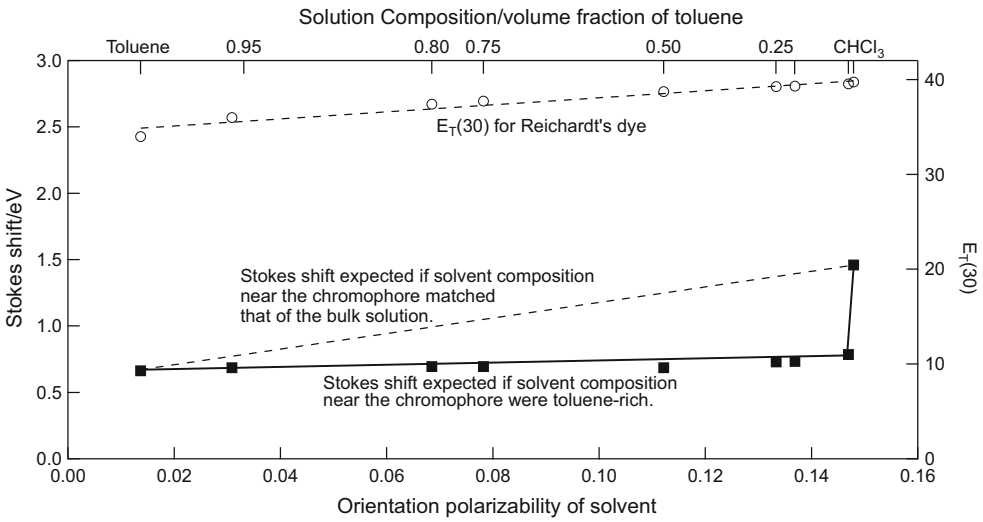


**Fig. 6** Stokes shifts for the $O_2$WPOSS complex dissolved in mixtures of toluene and chloroform. $E_T(30)$ for Reichardt's dye in the same solvent mixtures shown for reference (*upper line*)

partition constants yielded a value of about −28 kJ/mol for the apparent enthalpy of the preferential solvation. Therefore, we speculate that the preferentiality would attenuate ($K = 1$) at temperatures around 500 K. Because entropy of mixing would tend to cancel the preferential solvation, we considered the maximum entropy of mixing of a two-component system, which occurs for an equimolar mixture ($x_1 = x_2 = 0.5$). We estimate that the entropy of mixing would overwhelm the enthalpic term only at an impractically high temperature (~5000 K):

$$\begin{aligned} T\Delta S &= RT[x_1 \ln(x_1) + (1 - x_1)\ln(1 - x_1)] \\ T\Delta S_{\max} &= RT[0.5\ln(0.5) + (1 - 0.5)\ln(1 - 0.5)] \\ &= 8.314\,\mathrm{J\ mol^{-1}\ K^{-1}} \times 0.693 \times 5000\ \mathrm{K} \\ &= 29\ \mathrm{kJ\ mol^{-1}} \end{aligned} \quad (6)$$

A provocative extrapolation, given the relative contributions for enthalpy (strong) and entropy (weak), is that, the preferentiality would invert at higher temperatures, here higher than 500 K. The cybotactic region would then switch from being rich in nonpolar molecules to being rich in the polar species. Therefore the support optimization would depend on the degree of conversion (i.e., local concentration) as well as on local temperature.

In principle, therefore, for reactions like upgrading of biomass or Fischer–Tropsch synthesis, both of which necessarily involve mixtures of condensed polar and nonpolar products, the properties of a catalyst support could be tuned to optimize the near-catalyst composition of the reaction medium (Fig. 8), albeit only in condensed reaction medium because gases cannot be structured. Indeed, the recent construction of "Janus" particles [63, 64] appear to do just that.

The preferential solvation that we have reported above may arise from the interaction of the solvent molecules with the organic –R groups attached to the POSS complexes (akin to the support effect mooted above) rather than an affinity towards the chromophore itself. Regardless, the results provide evidence that solvatochromism can afford an indication of changes in composition of a condensed reaction medium located near a photo-responsive moiety similar to those found in catalysts based on transition metal oxides. We expect that interesting solvent effects will arise

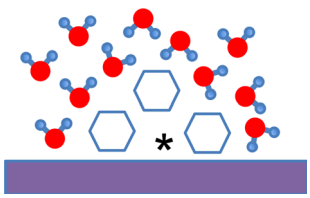


**Fig. 8** Cartoon representation of a support tuned to encourage preferential solvation near a catalytic site (*)

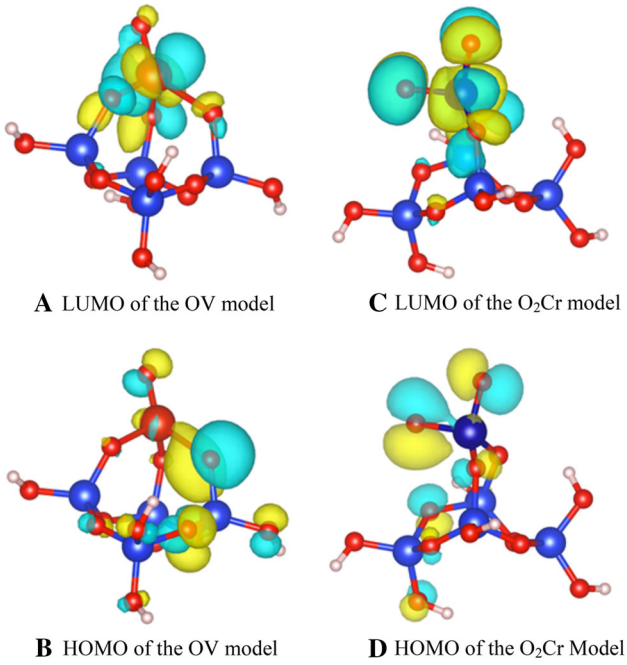


**Fig. 9** Frontier orbitals of the models of oxometalates, which show that the wavefunctions involved in the UV luminescence transitions are localized on the metal centers or their immediate neighbors

when there is charge separation in transition states and in reaction intermediates. For example, recent quantum calculations [65] that accord with experimental reaction selectivity [66] suggest that the preference for cyclohexanone over cyclohexanol in the hydrogenation of phenol in water likely arises from the presence of polarized intermediates stabilized by a polar reaction medium.

Many spectroscopies exhibit solvatochromism. We are aware that solvatochromism has also been observed in the IR spectroscopy of surface species [67, 68]. Here, we have chosen to employ UV solvatochromism because it probes, rather directly, the localized valence electronic properties of the chromophore (Fig. 9) and provides, and, as seen from the modest accordance between theory and experiment shown in Tables 1 and 2, a challenging benchmark to test the accuracy of modern quantum chemical calculations.

## 4 Conclusions

When a reaction medium consists only of highly miscible and similar components (e.g. when all are gases, or all are homologous hydrocarbons), questions about the local structure or composition of the reaction medium need not arise. In that case it is reasonable to assume that the molecules become well mixed normal to the surface of the

catalyst by ordinary random motion of the fluid phase species. However, in the upgrading of biomass-derived feedstocks into fuels, the ineluctable presence of polar as well as nonpolar liquids (e.g. water, oxygenates and the product fuel molecules) raises the possibility that stratification of the reaction medium can occur because there could be preferential interaction of one of the fluid phases with the catalyst surface or with pore walls. The results described above give reason to be concerned that such cybotactic stratification can exist, even in the nearly ideal solutions we employed.

The UV solvatochromic Stokes shifts of series of POSS-tethered oxometalate compounds in different neat solvents vary linearly with a measure of the solvent polarizability but exhibit significant preferential solvation in mixed solvents. TD-DFT calculations with simple models afforded semi-quantitative predictions at no great computational cost that can be transferred to extended model systems.

Knowledge of local concentrations, or better, activities [6], of reactants and products is needed to devise accurate rate laws and to improve the design of the surfaces of contact catalysts employed in condensed reaction media. The characterization technique exemplified here provides a way to probe that information. The technique is general and can be adapted to other, *in operando* spectroscopies, notably polarization decay spectroscopy, which can provide information about local solution dynamics, and resonant inelastic X-ray scattering (RIXS), which could be used in optically opaque media or under conditions of high temperature and pressure, for example in the recent study of unusual solvent effects during the hydrogenation of biogenic oxygenates [7].

**Acknowledgments** This research was supported in part by the Laboratory Directed Research & Development program at Pacific Northwest National Laboratory. PNNL is operated by Battelle for the US Department of Energy under contract DE-AC05-76RL01830. A portion of the research was performed at EMSL, a national scientific user facility sponsored by the Department of Energy's Office of Biological and Environmental Research and located at PNNL. This research also used resources of the National Energy Research Scientific Computing Center, which is supported by the Office of Science of the U.S. Department of Energy under Contract No. DE-AC02-05CH11231.

## Appendix

Here we present (1) the syntheses of the compounds we studied, (2) details of the spectroscopy of the OVPOSS samples, (3) an exemplary set of spectra showing the effect of solvents on the absorption and emission features, (4) estimations of the polarizabilities of the solvent mixtures, and (5) energies of the optical transitions calculated for the chromophores.

### Synthesis Protocols

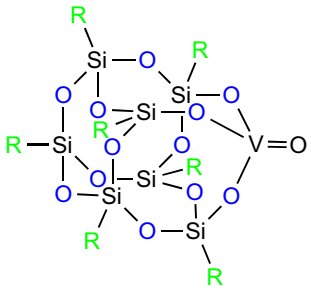


#### *OVPOSS Complex*

Two separate flasks were charged with starting materials under inert atmosphere, in the glove box, as follows: 0.172 g (1 mmol, 1 eq) of vanadyl (V) trichloride was charged in one flask, and 0.93 g of trisilanolphenyl POSS (1 mmol, 1 eq), was charged into a second flask. Anhydrous toluene was added to both flasks, inside the glove box. The POSS solution (20 mL) was added into the vanadyl solution (20 mL) with stirring. The resulting mixture was refluxed, and after 30 min of reflux, triethylamine (0.33 g) in 5 mL of toluene was added dropwise. The reaction mixture was allowed to reflux overnight (18 h). Next day, the precipitate formed was removed by filtration inside a glove box and the solution was stored in sealed vial inside a glove box. The solvent was not evaporated to prevent dimerization. In a second trial, vanadium oxytripropoxide was used as the vanadium source due to its superior stability as compared to vanadyl trichloride. A 3 mL solution of vanadium oxytripropoxide (0.25 mL, 1.10 mmol) in benzene, was added with vigorous stirring to a suspension of trisilanol phenyl POSS in benzene (1.00 g, 1.07 mmol). Complete dissolution of POSS was obtained in 5–10 min, however the reaction mixture was allowed to stir at room temperature overnight. The amorphous solid formed was isolated by filtration, while the benzene mother liquor was analyzed as is. The solution was characterized by $^{29}$Si NMR (three broad signals) and $^{51}$V NMR (−676 ppm). The presence of the signal at −676 ppm indicates the presence of symmetric $C_{3v}$ vanadyl species.

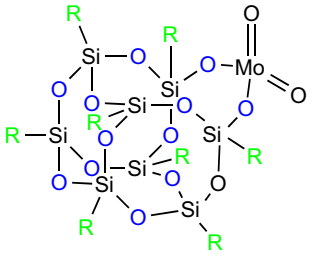

*$O_2$MoPOSS Complex*

Two separate flasks were charged with starting materials under inert atmosphere, in the glove box, as follows: 0.2 g (1 mmol) of molybdenum (VI) dichloride dioxide was charged in one flask, and 0.89 g of disilanolisobutyl POSS (1 mmol), was charged into a second flask. Anhydrous toluene was added to both flasks via cannula under argon, outside the glove box. The POSS solution (20 mL) was cannulated into the molybdenum solution (50 mL) with stirring. The resulting mixture was quickly brought to reflux, and after 30 min of reflux, triethylamine (0.33 g) in 5 mL of toluene was added dropwise. The resulting reaction mixture was refluxed for 18 h (overnight). Next day, the precipitate formed was removed by filtration in ambient atmosphere; the solid washed with dichloromethane and the filtrate was concentrated to an oil, which on standing crystallized. The yield was 0.5 g ($\sim$50 %). EIMS ($M^+$) *m/z*: 1017 (parent).

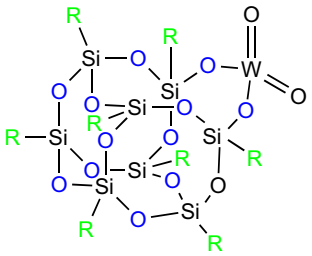

*$O_2$WPOSS Complex*

Two separate flasks were charged with starting materials under inert atmosphere, in the glove box, as follows: 0.16 g (0.56 mmol) of tungsten (VI) dichloride dioxide was charged in one flask, and 0.5 g of disilanolisobutyl POSS (0.56 mmol), was charged into a second flask. Anhydrous toluene was added to both flasks via cannula under argon, outside the glove box. The POSS solution (20 mL) was cannulated into the tungsten solution (50 mL) with stirring. The resulting mixture was quickly brought to reflux, and after 30 min of reflux, triethylamine (0.23 g) in 5 mL of toluene was added dropwise. The resulting reaction mixture was refluxed for 18 h (overnight). Next day, the precipitate formed was removed by filtration in ambient atmosphere, the solid washed with dichloromethane and the filtrate was concentrated to an oil, which on standing crystallized. The reaction is sluggish and thus yields are generally low and variable (average 10 %). The POSS can be removed to some extent by recrystallization from hexanes (POSS remains in mother liquor, while the complex precipitates out), and the mixture can be enriched in the $O_2$WPOSS desired product. EIMS ($M^+$) *m/z*: 1158 (Na salt of parent), 1124 (monohydrate of parent), 1044 (parent with loss of isobutyl group).

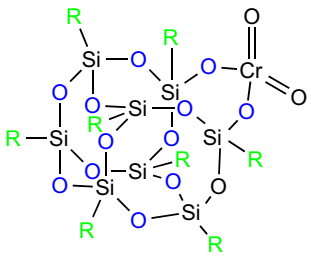

*Cr-POSS Complex*

A procedure analogous to that used to prepare the W-complex, was ineffective in the case of Cr. Instead, the Cr-POSS was prepared via a procedure of Feher and Blanski [49]. A round bottom flask was charged with disilanolisobutyl POSS (0.713 g, 0.8 mmol, 1 eq), $CrO_3$ (0.2 g) and $MgSO_4$ (0.5 g, dehydrating agent), under inert atmosphere in the glove box. To the solids, 30 mL $CCl_4$ were added, outside the glove box, via syringe, under argon, and the resulting slurry was stirred at room temperature overnight. The reaction mixture was sonicated the second day, three times for 30 min at 1-h intervals to ensure dispersion of $CrO_3$ in the mixture. During handling, the flask was wrapped in aluminum foil to protect the contents from light. The solvent was then removed under reduced pressure, the solid was suspended in acetone and removed by filtration. The filtrate was concentrated to yield an amorphous orange-red glassy solid (38 mg, 5 % yield). EIMS ($M^+$) *m/z*: 991 (hydrate of parent), 971 (parent compound).

## Spectroscopy of OVPOSS Samples

OVPOSS is not stable as a monovanadium complex [49]. The more stable dimer readily forms in solution and that propensity increases with increasing concentration. This is especially true for our investigation where the solutions are

prepared by dissolving solid 'OVPOSS' as opposed to studying in situ reaction solutions. A series of absorption measurements was used to determine the absorption maximum ($\lambda_{abs}$) of the monomer and the dimer. Both complexes coexisted at all conditions, but the assumption underlying the experiment was that predominantly the dimer exists in solution as the concentration is increased, while the percentage of monomer increases at lower concentrations. The absorption peak, $\lambda_{abs}$, of the monomer was subsequently used as the excitation wavelength for emission measurements of differently concentrated OVPOSS containing solutions. The emission peak ($\lambda_{em}$) of the monomer and the dimer are distinctly different (separated by $\sim$1 eV) with the monomer emitting light at lower energy. Throughout this study we exclusively report $\lambda_{abs}$ and $\lambda_{em}$ of the monomer. Except for the complication of having two photoactive species in solution, the measurements were identical to the procedure described in the main text.

## Solvatochromism of $O_2$WPOSS

The solvent composition appeared to mostly affect the position of the emission maximum, exemplified below with the $O_2$WPOSS complex in chloroform/toluene mixtures. See Fig. 10.

## Orientation Polarizabilities of the Mixtures

We have used the following definition of, $\Delta f$:

$$\Delta f = \frac{\varepsilon - 1}{2\varepsilon + 1} - \frac{n^2 - 1}{2n^2 + 1}.$$

We measured the indices of refraction of the mixtures, *n,* but approximated the relative permittivities, ε, using the mixing rules described by Wang and Anderko [52]. See Table 3.

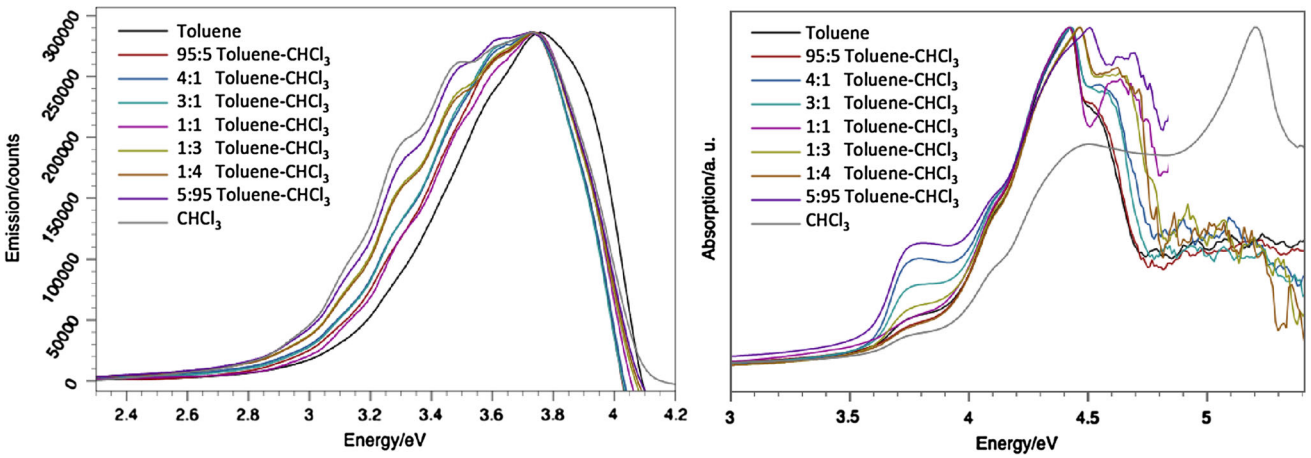


**Fig. 10** UV–Visible spectra of $O_2$WPOSS in mixtures of toluene and chloroform. *Left* emission spectra excited at (280 nm = 4.43 eV), *Right* absorption spectra

**Table 3** Measured refractive index and calculated permittivity and orientation polarizibility

| Solution (volume fraction of first component) | Index of refraction, *n* (measured) | Relative permittivity, ε (Calculated) | Orientation Polarizability, $\Delta f$ |
|---|---|---|---|
| Toluene:Chloroform (1.00) | 1.4955 | 2.380 | 0.0136 |
| Toluene:Chloroform (0.80) | 1.4861 | 2.099 | 0.0685 |
| Toluene:Chloroform (0.75) | 1.4824 | 3.253 | 0.0782 |
| Toluene:Chloroform (0.50) | 1.4685 | 3.907 | 0.112 |
| Toluene:Chloroform (0.25) | 1.4567 | 4.411 | 0.133 |
| Toluene:Chloroform (0.20) | 1.454 | 4.498 | 0.137 |
| Toluene:Chloroform (0.00) | 1.4439 | 4.810 | 0.149 |
| Tetrahydrofuran (1.00) | 1.4072 | 7.580 | 0.161 |

**Table 4** Calculated optical transition energies, all in eV

| Chromophore | Vertical absorption | | Emission | | Calc. stokes shift | | Expt. stokes shift | |
|---|---|---|---|---|---|---|---|---|
| | Toluene | Chloroform | Toluene | Chloroform | Toluene | Chloroform | Toluene | Chloroform |
| OV | 4.74 | 4.74 | 1.8 | 2.1 | 2.94 | 2.64 | 2.249 | 2.743 |
| $O_2Cr$ | 4.1 | 4.29 | 2.5 | 2.74 | 1.6 | 1.55 | 1.39 | 2.795 |
| $O_2Mo$ | 5 | 5 | 2.78 | 2.7 | 2.22 | 2.3 | 0.992 | 2.163 |
| $O_2W$ | 5.2 | 5 | 2.9 | 2.85 | 2.3 | 2.15 | 0.663 | 1.715 |

| Chromophore | Diagonal absorption | | Emission | | Calc. stokes shift | |
|---|---|---|---|---|---|---|
| | Toluene | Chloroform | Toluene | Chloroform | Toluene | Chloroform |
| OV | 3.88 | 3.9 | 1.8 | 2.1 | 2.08 | 1.8 |
| $O_2Cr$ | 3.04 | 2.74 | 2.5 | 2.74 | 0.54 | 0 |
| $O_2Mo$ | 3.92 | 3.9 | 2.78 | 2.7 | 1.14 | 1.2 |
| $O_2W$ | 4.26 | 5.52 | 2.9 | 2.85 | 1.36 | 2.67 |

## Calculated Optical Transition Energies

The table below presents the energies in eV for the HOMO–LUMO and LUMO–HOMO transitions for the clusters containing the indicated chromophores. Vertical transitions evaluate the energy of promoting (or relaxing) a single electron transfer between energy levels evaluated in the geometry of the starting state. Diagonal transitions evaluate the transition energy between geometry-optimized starting and final states. See Table 4.

## References


1. Boudart M, Cheng WC (1987) Catalytic hydrogenation of cyclohexene: 7. Liquid phase reaction on supported nickel. J Catal 106(1):134–143
2. Clerici MG (2001) The role of the solvent in TS-1 chemistry: active or passive? An early study revisited. Top Catal 15(2–4):257–263
3. Mukherjee S, Vannice M (2006) Solvent effects in liquid-phase reactions I. Activity and selectivity during citral hydrogenation on Pt/SiO2 and evaluation of mass transfer effects. J Catal 243(1):108–130. doi:10.1016/j.jcat.2006.06.021
4. Mukherjee S, Vannice M (2006) Solvent effects in liquid-phase reactions II. Kinetic modeling for citral hydrogenation. J Catal 243(1):131–148. doi:10.1016/j.jcat.2006.06.018
5. Singh UK, Vannice MA (2001) Kinetics of liquid-phase hydrogenation reactions over supported metal catalysts—a review. Appl Catal A 213(1):1–24
6. Madon RJ, Iglesia E (2000) Catalytic reaction rates in thermodynamically non-ideal systems. J Mol Catal A 163:189–204
7. Wan H, Vitter A, Chaudhari RV, Subramaniam B (2014) Kinetic investigations of unusual solvent effects during Ru/C catalyzed hydrogenation of model oxygenates. J Catal 309:174–184
8. Wan H, Chaudhari RV, Subramaniam B (2012) Catalytic hydroprocessing of p-Cresol: metal, solvent and mass-transfer effects. Top Catal 55(3–4):129–139
9. Struijk J, Scholten J (1992) Selectivity to cyclohexenes in the liquid phase hydrogenation of benzene and toluene over ruthenium catalysts, as influenced by reaction modifiers. Appl Catal A 82(2):277–287
10. Román-Leshkov Y, Dumesic JA (2009) Solvent effects on fructose dehydration to 5-hydroxymethylfurfural in biphasic systems saturated with inorganic salts. Top Catal 52(3): 297–303
11. Caratzoulas S, Davis ME, Gorte RJ, Gounder R, Lobo RF, Nikolakis V, Sandler SI, Snyder MA, Tsapatsis M, Vlachos DG (2014) Challenges of and insights into acid-catalyzed transformations of sugars. J Phys Chem C 118:22815–22833
12. Reichardt C (1982) Solvent effects on chemical reactivity. Pure Appl Chem 54:1867–1884
13. Reichardt C, Welton T (2010) Solvent effects in organic chemistry, 4th edn. Wiley-VCH, Weinheim
14. Buncel E, Stairs RA, Wilson H (2003) The role of the solvent in chemical reactions. Oxford University Press, Oxford
15. Jessop PG, Jessop DA, Fu D, Phan L (2012) Solvatochromic parameters for solvents of interest in green chemistry. Green Chem 14(5):1245–1259. doi:10.1039/c2gc16670d
16. Marini A, Muñoz-Losa A, Biancardi A, Mennucci B (2010) What is Solvatochromism? J Phys Chem B 114(51):17128–17135
17. Fidale LC, Heinze T, El Seoud OA (2013) Perichromism: a powerful tool for probing the properties of cellulose and its derivatives. Carbohydr Polym 93:129–134
18. Grate JW, Zhang C, Wietsma TW, Warner MG, Anheier NC, Bernacki BE, Orr G, Oostrom M (2010) A note on the visualization of wetting film structures and a nonwetting immiscible fluid in a pore network micromodel using a solvatochromic dye. Water Resour Res 46(11):W11602/11601–W11602/11606
19. Zhang X, Steel WH, Walker RA (2003) Probing solvent polarity across strongly associating solid/liquid interfaces using molecular rulers. J Phys Chem B 107:3829–3836
20. Michaelis J, Braeuchle C (2010) Reporters in the nanoworld: diffusion of single molecules in mesoporous materials. Chem Soc Rev 39(12):4731–4740. doi:10.1039/c0cs00107d
21. Anpo M, Matsuoka M, Takeuchi M (2009) Photofunctional zeolites and mesoporous materials incorporating single-site heterogeneous catalysts. In: Klabunde KJ, Richards RM (eds) Nanoscale materials in chemistry, 2nd edn. Wiley, New York, pp 605–627
22. Hazenkamp M, Blasse G (1992) Characterization of silica supported transition-metal oxide catalysts by luminescence spectroscopy. Ber Bunsen Ges 96(10):1471–1477
23. Hazenkamp M, Blasse G (1992) A luminescence spectroscopy study on supported vanadium and chromium-oxide catalysts. J Phys Chem 96(8):3442–3446

24. Lee EL, Wachs IE (2008) Molecular design and in situ spectroscopic investigation of multilayered supported $M_1O_x/M_2O_x/SiO_2$ catalysts. J Phys Chem C 112:20418–20428
25. Lewandowska AE, Banares MA, Tielens F, Che M, Dzwigaj S (2010) Different kinds of tetrahedral V species in vanadium-containing zeolites evidenced by diffuse reflectance UV–Vis, Raman, and periodic density functional theory. J Phys Chem C 114:19771–19776
26. Mota A, Hallett JP, Kuznetsov ML, Correia I (2011) Structural characterization and DFT study of VIVO(acac)2 in imidazolium ionic liquids. Phys Chem Chem Phys 13(33):15094–15102. doi:10.1039/c1cp20800d
27. Weckhuysen B, Keller D (2003) Chemistry, spectroscopy and the role of supported vanadium oxides in heterogeneous catalysis. Catal Today 78:25–46
28. Adolph S, Spange S, Zimmerman Y (2000) Catalytic activities of various moderately strong solid acids and their correlation with surface polarity parameters. J Phys Chem B 104:6429–6438
29. Kahle I, Spange S (2010) Internal and external acidity of faujasites as measured by a solvatochromic spiropyran. J Phys Chem C 114:15448–15453
30. Prause S, Spange S (2004) Adsorption of polymers on inorganic solid acids investigated by means of coadsorbed solvatochromic probes. J Phys Chem B 108:5734–5741
31. Seifert S, Seifert A, Brunklaus G, Hofmann K, Rüffer T, Lang H, Spange S (2012) Probing the surface polarity of inorganic oxides using merocyanine-type dyes derived from barbituric acid. New J Chem 36:674–684
32. Spange S, Vilsmeier E, Zimmerman Y (2000) Probing the surface polarity of various silicas and other moderately strong solid acids by means of different genuine solvatochromic dyes. J Phys Chem B 104:6417–6428
33. Spange S, Zimmerman Y, Graeser A (1999) Hydrogen-bond-donating acidity and dipolarity/polarizability of surfaces with silica gels and mesoporous MCM-41 materials. Chem Mater 11:3245–3251
34. Zhang X, Cunningham MM, Walker RA (2003) Solvent polarity at polar solid surfaces: the role of solvent structure. J Phys Chem B 107:3183–3195
35. Mudring A-V, Kirchner B (2009) Optical spectroscopy and ionic liquids. Top Curr Chem 290:285–310. doi:10.1007/128_2008_45
36. Ravi M, Samanta A, Radhakrishnan TP (1994) Excited state dipole moments from an efficient analysis of solvatochromic stokes shift data. J Phys Chem 98:9133–9136
37. Schoonheydt RA (2010) UV-VIS-NIR spectroscopy and microscopy of heterogeneous catalysts. Chem Soc Rev 39(12):5051–5066. doi:10.1039/c0cs00080a
38. Silva PL, Trassi MAS, Martins CT, El Seoud OA (2009) Solvatochromism in binary mixtures: first report on a solvation free energy relationship between solvent exchange equilibrium constants and the properties of the medium. J Phys Chem B 113:9512–9519
39. Lakowicz JR (1999) Principles of fluorescence spectroscopy, vol 1, vol 6, 2nd edn., Solvent effects on emission spectra. Kluwer Academic Publishers, New York, p 187
40. Quadrelli EA, Basset J-M (2010) On silsesquioxanes' accuracy as molecular models for silica-grafted complexes in heterogeneous catalysis. Coord Chem Rev 254(5–6):707–728. doi:10.1016/j.ccr.2009.09.031
41. Yoon CW, Hirsekorn KF, Neidig ML, Yang X, Tilley TD (2011) Mechanism of the decomposition of aqueous hydrogen peroxide over heterogeneous TiSBA15 and TS-1 selective oxidation catalysts: insights from spectroscopic and density functional theory studies. ACS Catalysis 1:1665–1678
42. Feher FJ, Blanski RL (1990) Polyhedral oligometallasilasesquioxanes as models for silica-supported catalysts: chromium attached to two vicinal siloxy groups. J Chem Soc, Chem Commun 22:1972–1995
43. Cabrero-Antonino JR, García T, Rubio-Marqués P, Vidal-Moya JA, Leyva-Pérez A, Al-Deyab SS, Al-Resayes SI, Díaz U, Corma A (2011) Synthesis of organic–inorganic hybrid solids with copper complex framework and their catalytic activity for the S-arylation and the azide–alkyne cycloaddition reactions. ACS Catalysis 1(2):147–158. doi:10.1021/cs100086y
44. Lu C, Chang F (2011) Polyhedral oligomeric silsesquioxane-encapsulating amorphous palladium nanoclusters as catalysts for heck reactions. ACS Catalysis 1:481–488
45. Groppo E, Lamberti C, Bordiga S, Spoto G, Zecchina A (2005) The structure of active centers and the ethylene polymerization mechanism on the Cr/SiO2 catalyst: a frontier for the characterization methods. Chem Rev 105(1):115–184. doi:10.1021/cr040083s
46. Wachs IE, Routray K (2012) Catalysis science of bulk mixed oxides. ACS Catalysis 2(6):1235–1246. doi:10.1021/cs2005482
47. Copéret C (2007) Design and understanding of heterogeneous alkene metathesis catalysts. J Chem Soc Dalton Trans 47:5498–5504
48. Anpo M, Kim T-H, Matsuoka M (2009) The design of Ti-, V-, Cr-oxide single-site catalysts within zeolite frameworks and their photocatalytic reactivity for the decomposition of undesirable molecules—The role of their excited states and reaction mechanisms. Catal Today 142(3–4):114–124
49. Feher FJ, Walzer JF (1991) Synthesis and characterization of vanadium-containing silsesquioxanes. Inorg Chem 30(8):1689–1694
50. Wada K, Itayama N, Watanabe N, Bundo M, Kondo T, T-a Mitsudo (2004) Synthesis and catalytic activity of group 4 metallocene containing silsesquioxanes bearing functionalized silyl groups. Organometallics 23(24):5824–5832
51. Wada K, Nakashita M, Yamamoto A, Wada H, Mitsudo T (1998) Activities of polyhedral vanadium-containing silsesquioxane-based catalysts for photo-assisted oxidation of hydrocarbons. Res Chem Intermed 24(5):515–527
52. Wang P, Anderko A (2001) Computation of dielectric constants of solvent mixtures and electrolyte solutions. Fluid Phase Equilib 186:103–122
53. Ernzerhof M, Perdew PJ (1998) Generalized gradient approximation to the angle- and system-averaged exchange hole. J Chem Phys 109:3313–3320
54. Adamo C, Barone V (2000) Inexpensive and accurate predictions of optical excitations in transition-metal complexes: the TDDFT/PBE0 route. Theor Chem Acc 105:169–172
55. Scalmani G, Frisch MJ, Mennucci B, Tomasi J, Cammi R, Barone V (2006) Geometries and properties of excited states in the gas phase and in solution: theory and application of a time-dependent density functional theory polarizable continuum model. J Chem Phys 124(094107):1–15
56. Frisch MJ, Trucks GW, Schlegel HB, Scuseria GE, Robb MA, Cheeseman JR, Scalmani G, Barone V, Mennucci B, Petersson GA, Nakatsuji H, Caricato M, Li X, Hratchian HP, Izmaylov AF, Bloino J, Zheng G, Sonnenberg JL, Hada M, Ehara M, Toyota K, Fukuda R, Hasegawa J, Ishida M, Nakajima T, Honda Y, Kitao O, Nakai H, Vreven T, Montgomery JA, Jr., Peralta JE, Ogliaro F, Bearpark M, Heyd JJ, Brothers E, Kudin KN, Staroverov VN, Kobayashi R, Normand J, Raghavachari K, Rendell A, Burant JC, Iyengar SS, Tomasi J, Cossi M, Rega N, Millam NJ, Klene M, Knox JE, Cross JB, Bakken V, Adamo C, aramillo J, Gomperts R, Stratmann RE, Yazyev O, Austin AJ, Cammi R, Pomelli C, Ochterski JW, Martin RL, Morokuma K, Zakrzewski VG, Voth GA, Salvador P, Dannenberg JJ, Dapprich S, Daniels AD, Farkas Ö, Foresman JB, Ortiz JV, Cioslowski J, Fox DJ (2009) Gaussian 09 Revision D.01. Gaussian Inc., Wallingford

57. Tomasi J, Mennucci B, Cammi R (2005) Quantum mechanical continuum solvation models. Chem Rev 105:2999–3093
58. Furche F, Rappoport D (2005) Density functional methods for excited states: equilibrium structure and electronic spectra. In: Olivucci M (ed) Theoretical and computational chemistry, vol 16. Elsevier, Amsterdam, pp 93–128
59. Bosch E, Rived F, Rosés M (1996) Solute-solvent and solvent-solvent interactions in binary solvent mixtures. Part 4. Preferential solvation of solvatochromic indicators in mixtures of 2-methylpropan-2-ol with hexane, benzene, propan-2-ol, ethanol and methanol. J Chem Soc Perkin Trans 2(2):2177–2184
60. Reid RC, Prausnitz JM, Sherwood TK (1977) The properties of gases and liquids. Their estimation and correlation. McGraw-Hill, New York
61. Marcus Y (1994) Use of chemical probes for the characterization of solvent mixtures. Part 1. Completely non-aqueous mixtures. J Chem Soc Perkin Trans 2:1015–1021
62. Marcus Y (1994) The use of chemical probes for the characterization of solvent mixtures. Part 2. Aqueous mixtures. J Chem Soc Perkin Trans 2:1751–1758
63. Crossley S, Faria J, Shen M, Resasco DE (2010) Solid nanoparticles that catalyze biofuel upgrade reactions at the water/oil interface. Science 327:68–72
64. Shen M, Resasco DE (2009) Emulsions stabilized by carbon nanotube–silica nanohybrids. Langmuir 25:10843–10851
65. Yoon Y, Rousseau R, Weber RS, Lercher JA (2014) First-principles study of phenol hydrogenation on Pt and Ni catalysts in aqueous phase. J Am Chem Soc 136:10287–10298
66. Zhao C, He J, Lemonidou AA, Li X, Lercher JA (2011) Aqueous-phase hydrodeoxygenation of bio-derived phenols to cycloalkanes. J Catal 280:8–16
67. Wang H, Borguet E, Eisenthal KB (1997) Polarity of liquid interfaces by second harmonic generation spectroscopy. J Phys Chem A 101(4):713–718
68. Wang H, Borguet E, Eisenthal KB (1998) Generalized interface polarity scale based on second harmonic spectroscopy. J Phys Chem B 102(25):4927–4932